HIV-1 accessory protein Vpr interacts with REAF/RPRD2 to mitigate its antiviral activity.

Joseph M Gibbons[a], Kelly M Marno[a], Rebecca Pike[a], Wing-yiu Jason Lee[a], Christopher E Jones[a], Babatunji W Ogunkolade[a], Claire Pardieu[a], Alexander Bryan[b], Rebecca Menhua Fu[b], Gary Warnes[a], Paul A Rowley[c], Richard D Sloan[b,d] and Áine McKnight[a#]

[a]The Blizard Institute, Queen Mary University of London School of Medicine and Dentistry, QMUL, UK.

[b]Infection Medicine, The University of Edinburgh, UK.

[c]Department of Biological Sciences, The University of Idaho, Moscow, Idaho, USA.

[d]ZJU-UoE Institute, Zhejiang University, P.R. China.

Running Head: Vpr mitigates REAF/RPRD2

Address correspondence to Áine McKnight, a.mcknight@qmul.ac.uk.

K.M.M and R.P contributed equally to this work.

Abstract

The Human Immunodeficiency Virus type 1 (HIV-1) accessory protein Vpr enhances viral replication in both macrophages and in cycling T cells to a lesser extent. Virion packaged Vpr is released in target cells shortly after entry, suggesting its requirement in the early phase of infection. Previously, we described REAF (RNA-associated Early-stage Antiviral Factor, RPRD2), a constitutively expressed protein that potently restricts HIV replication at or during reverse transcription. Here, we show that a virus without intact *vpr* is more highly restricted by REAF and, using delivery by VLPs, that Vpr alone is sufficient for REAF degradation in primary macrophages. REAF is more highly expressed in macrophages than in cycling T cells and we detect, by co-immunoprecipitation assay, an interaction between Vpr protein and endogenous REAF. Vpr acts very quickly during the early phase of replication and induces the degradation of REAF within 30 minutes of viral entry. Using Vpr F34I and Q65R viral mutants, we show that nuclear localisation and interaction with cullin4A-DBB1 (DCAF1) E3 ubiquitin ligase is required for REAF degradation by Vpr. In response to infection, cells upregulate REAF levels. This response is curtailed in the presence of Vpr. These findings support the hypothesis that Vpr induces the degradation of a factor, REAF, which impedes HIV infection in macrophages.

Importance

For at least 30 years, it has been known that HIV-1 Vpr, a protein carried in the virion, is important for efficient infection of primary macrophages. Vpr is also a determinant of the pathogenic effects of HIV-1 *in vivo.* A number of cellular proteins that interact with Vpr have been identified. So far, it has not been possible to associate these proteins with altered viral replication in macrophages, or to explain why Vpr is carried in the virus particle. Here we show that Vpr

mitigates the antiviral effects of REAF, a protein highly expressed in primary macrophages and one which inhibits virus replication early during reverse transcription. REAF is degraded by Vpr within 30 minutes of virus entry, in a manner dependent on the nuclear localization of Vpr and its interaction with the cell's protein degradation machinery.

75 ## Introduction

76 Human Immunodeficiency Virus type 1 (HIV-1) infects $CD4^+$ T cells and macrophages *in*
77 *vivo*. HIV-1 has four non-structural accessory genes *nef*, *vif*, *vpu* and *vpr*. *Nef, vif and vpu* diminish
78 host innate immunity. A function for Vpr has been elusive, but it is required for efficient replication
79 in macrophages and for pathogenesis *in vivo* (1, 2). A widely acknowledged but poorly understood
80 Vpr-mediated phenotype is that it induces cell cycle arrest at the G2/M phase using the cullin4A-
81 DBB1 (DCAF1) E3 ubiquitin ligase and the recruitment of an unknown substrate for proteasomal
82 degradation. A large number of Vpr substrates have been reported (3-11). Yan *et al.* (2019) show
83 that helicase-like transcription factor (HLTF) weakly restricts replication of HIV-1 in T cells.
84 HLTF was shown previously to be down modulated by Vpr (12, 13). Furthermore, Greenwood *et*
85 *al.* 2019 report that Vpr promotes large scale remodelling of approximately 2000 cellular proteins,
86 including those that bind nucleic acids and ones involved with the cell cycle (14).

87 Substantial quantities of Vpr are incorporated into viral particles and released from the
88 major capsid protein (CA) after entry into the cell (15, 16). The timing of Vpr release coincides
89 with the initiation of reverse transcription, a process that transcribes the RNA genome into DNA
90 for subsequent integration into the host cell DNA (17). The early release of Vpr from the CA
91 implies it has an early function prior to integration events. When considering the role of Vpr in
92 cell tropism and pathogenesis, the investigation of proteins that have a direct effect on viral
93 replication is a priority.

94 Here we focus on RNA-associated Early-stage Antiviral Factor (REAF, also known as
95 Regulation of nuclear pre-mRNA domain-containing protein 2/RPRD2), originally described as a
96 restriction to HIV replication and called lentiviral restriction 2 (Lv2) (18, 19). Lv2 was first shown
97 to be a restriction to the replication of HIV-2 and subsequently it was shown to inhibit the

98 replication of HIV-1 and SIV during reverse transcription (20). Lv2/REAF restriction is cell type
99 dependent (19, 21-24), active in certain cell types including HeLa-CD4 and primary macrophages
100 (18, 19). Susceptibility of the virus to Lv2 is determined by both the viral envelope (Env) and
101 capsid (CA) (23, 24). REAF was identified in a whole genome siRNA screen for the identification
102 of HIV-1 restriction factors. Like Lv2, REAF limits the completion of proviral DNA synthesis and
103 integration of the viral genome (18). Subsequently, REAF was demonstrated to form a major
104 component of Lv2 (19).

105 Here, we show that within 30 minutes of cellular entry, only HIV-1 virus that contains Vpr
106 can induce the degradation of REAF and rescue efficient viral replication in primary macrophages.
107 Using Vpr mutant viruses, we demonstrate that the nuclear localisation of Vpr, and its ability to
108 interact with cullin4A-DBB1 (DCAF1) E3 ubiquitin ligase, is a requirement for REAF
109 degradation. Down modulation of REAF by Vpr in the early phase of infection is transient and re-
110 expression to basal levels is achieved by approximately one hour. After infection with HIV-1, or
111 treatment with polyriboinosinic:polyribocytidylic acid (poly(I:C)) or Lipopolysaccharide (LPS),
112 cells respond by increasing REAF levels. In the case of viral infection, this response is curtailed
113 in the presence of Vpr. Therefore, our results support the hypothesis that Vpr induces the
114 degradation of a cellular protein, REAF, a protein which impedes HIV-1 infection in macrophages
115 during reverse transcription.

116

117

118

119

120

121 ## Results

122 **HIV-1 Vpr interacts with REAF and overcomes restriction.**

123 REAF restricts HIV-1 replication in HeLa-CD4 (18, 20). We sought to determine if a viral
124 accessory gene could overcome REAF and so we tested the infectivity of HIV-1 89.6^{WT} and
125 mutants deleted for *vpr* ($89.6^{\Delta vpr}$), *vif* ($89.6^{\Delta vif}$) or *vpu* ($89.6^{\Delta vpu}$) in these cells. Preventing REAF
126 expression using short-hairpin RNA (HeLa-CD4 shRNA-REAF, Figure 1A) reveals its potent
127 antiviral effect. Despite a standard input for each virus (50 FFU/ml, as measured on HeLa-CD4),
128 there is significantly greater rescue of HIV-1 $89.6^{\Delta vpr}$ (>3 fold, $p < 0.0001$) compared to HIV-1
129 89.6^{WT} (Figure 1B). The prevention of REAF expression using shRNA alleviates the need for Vpr.
130 Conversely, there was no significantly greater rescue for either HIV-1 $89.6^{\Delta vif}$ or HIV-1 $89.6^{\Delta vpu}$
131 compared to HIV-1 89.6^{WT} (data not shown). Thus, *vpr* potently overcomes the restriction imposed
132 by REAF.

133 We are unaware of previous reports that Vpr overcomes known or unknown HIV-1
134 restrictions in HeLa-CD4. Therefore, we confirmed that the mutant HIV-1 $89.6^{\Delta vpr}$ is restricted in
135 HeLa-CD4 compared to HIV-1 89.6^{WT}. Figure 1C shows that despite equal viral inputs (measured
136 by ELISA of viral protein p24), significantly fewer foci of infection (FFU) result from challenge
137 with HIV-1 $89.6^{\Delta vpr}$ compared to HIV-1 89.6^{WT}. Further support of a role for Vpr in overcoming
138 REAF is evidenced in Figure 1D. When HeLa-CD4 are challenged with a HIV-1 89.6^{WT} (which
139 has an intact *vpr*), REAF protein is down modulated. The observed down modulation is dependent
140 on the presence of Vpr as HIV-1 $89.6^{\Delta vpr}$ is incapable of degrading REAF. Moreover, Figure 1E
141 shows that Vpr and REAF interact with each other, either directly or indirectly as part of a
142 complex, as they are co-immunoprecipitated.

143 Vpr is released from the capsid and enters the nucleus shortly after infection (11). Imaging

144 flow cytometry combines traditional flow cytometry with microscopy, facilitating the evaluation
145 of both the expression and subcellular localisation of proteins in large populations of cells (25, 26).
146 Using imaging flow cytometry, we determined the relative subcellular localization of REAF in
147 HeLa-CD4. This analysis reveals that REAF is more highly expressed in the nuclear region
148 compared to the cytoplasmic region of cycling HeLa-CD4 (Figure 1F).

149 Previously, we reported that REAF affects the production of reverse transcripts early in
150 infection and that at this critical time point, REAF is transiently down modulated in HeLa-CD4
151 (20). Also using image flow cytometry, we looked the subcellular distribution of REAF at the early
152 time points following HIV-1 infection. Here, REAF protein was quantified by imaging flow
153 cytometry in the cytoplasm and nucleus of HeLa-CD4 over the first 3 hours of infection with
154 either HIV-1 89.6^{WT} or HIV-1 $89.6^{\Delta vpr}$. Following challenge with HIV-1 $89.6^{\Delta vpr}$, REAF levels
155 increase within 0.5 hours in both the nucleus (~25%, Figure 1G, left) and cytoplasm (~10%, Figure
156 1G, right). Nuclear levels remain high for 3 hours. Conversely, in the presence of Vpr (HIV-1
157 89.6^{WT}) this increase in REAF is curtailed, instead there is a steady decline from 0.5-2 hours. The
158 decline is most apparent in the nucleus with ~20% reduction by 1 hour and ~30% at 2 hours. By 3
159 hours, levels of REAF protein recover. The virus carries limited quantities of Vpr (17), which
160 potentially explains why there is a pause in REAF down modulation. Lower levels of REAF were
161 also observed in the cytoplasm over time after infection with HIV-1 89.6^{WT}, but to a much lesser
162 extent (Figure 1G, right). The nuclear enrichment score (NES) is a comparison of the intensity of
163 REAF fluorescence inside the nucleus (defined using DAPI) to the total fluorescence intensity of
164 REAF in the entire cell (defined using brightfield images). The lower the score, the less REAF in
165 the nucleus relative to in the cell overall. Imaging flow cytometry software determined the NES
166 over time after infection with HIV-1 89.6^{WT} or HIV-1 $89.6^{\Delta vpr}$ (Figure 1H). By 1-2 hours, a

167 significant segregation emerges; in the presence of Vpr relative nuclear levels of REAF are
168 suppressed. The greatest segregation occurs 2 hours post infection.
169
170 **Fluctuations in subcellular REAF expression after HIV-1 infection are Vpr dependent.**
171 Macrophages are a target for HIV infection *in vivo* (27). Vpr has been shown, to varying
172 degrees, to be more beneficial for replication in these cells than in cycling T cells (28-32). For that
173 reason, we investigated REAF effects in monocyte-derived macrophages (MDMs). Also using
174 imaging flow cytometry, we determined that similar to HeLa-CD4, MDMs have significantly
175 greater quantities of REAF in the nucleus compared to in the cytoplasm (Figure 2A). Nuclear
176 levels of REAF were also compared in a number of primary cell types using imaging flow
177 cytometry (Figure 2B). When compared with either monocytes or resting/activated T cells, both
178 MDMs and dendritic cells (DCs) highly express nuclear REAF. In Figure 2C, MDMs were treated
179 with virus-like particles (VLPs) containing Vpr and Western blotting confirmed that Vpr down
180 modulates REAF in MDMs and that Vpr alone is sufficient to induce this down modulation.
181 We investigated the ability of Vpr to degrade REAF in MDMs early in infection. The
182 subcellular fluctuations in REAF mean fluorescence intensity (MFI) were measured by imaging
183 flow cytometry in large populations of target cells (>5000). In the presence of Vpr (HIV-1 89.6^{WT}),
184 nuclear REAF decreases within 2 hours of viral infection of macrophages from two donors (Figure
185 2D), similar to that observed in HeLa-CD4 (Figure 1G). In contrast, also in both donors, nuclear
186 REAF rapidly increases from as early as 0.5 hours when the virus does not contain Vpr (HIV-1
187 $89.6^{\Delta vpr}$) (Figure 2D). For the cytoplasmic compartment, a similar picture emerges for REAF
188 fluctuation. In both donors, when Vpr is absent, REAF levels increase rapidly within 0.5 hours of
189 infection (Figure 2D). This cytoplasmic increase is curtailed in donor 1 when Vpr is present. In

190 donor 2, the loss of nuclear REAF after HIV-1 89.6^{WT} infection is paralleled by an increase in
191 cytoplasmic REAF. Similar kinetics of *total* REAF protein fluctuation were measured by Western
192 blotting in the presence or absence of Vpr in MDMs from two further donors (data not shown).

193 We sought to determine if knockdown of REAF in primary macrophages results in an
194 increase in susceptibility to HIV-1 infection. In Figure 2E, primary MDMs were treated with
195 siRNA targeting REAF (siREAF) or a control protein (siCB). Cells lacking REAF were found to
196 be significantly ($p<0.0001$) more susceptible to infection with HIV-1 89.6. We confirmed previous
197 reports that HIV-1 replication in MDMs is more efficient in the presence of Vpr (27, 30). Figure
198 2F shows that HIV-1 $89.6^{\Delta vpr}$ has restricted replication in MDMs compared with the wild type
199 virus expressing Vpr (HIV-1 89.6^{WT}).

200 To investigate further the relationship between nuclear REAF and Vpr, we generated a
201 virus with a substitution within Vpr (F34I). HIV-1 89.6^{F34I} is incapable of localising to the nuclear
202 membrane or of interacting with the nuclear transport protein importin-α and nucleoporins (30).
203 Like HIV-1 $89.6^{\Delta vpr}$, the mutant virus (HIV-1 89.6^{F34I}) replicates less efficiently in MDMs (Figure
204 2F). Using imaging flow cytometry, the respective abilities of these three viruses (HIV-1 89.6^{WT},
205 $89.6^{\Delta vpr}$ and 89.6^{F34I}) in down modulating total REAF protein was investigated in MDMs (Figure
206 2G). As expected, there is a loss of total REAF from 30 minutes after HIV-1 89.6^{WT} infection
207 (Figure 2G) with a transient recovery at around 2 hours. The opposite occurs in the absence of Vpr
208 (HIV-1 $89.6^{\Delta vpr}$), REAF levels *increase* after infection. The increase in REAF levels is most potent
209 after 30 minutes of infection with HIV-1 $89.6^{\Delta vpr}$. HIV-1 89.6^{F34I}, similar to HIV-1 $89.6^{\Delta vpr}$ can
210 no longer deplete REAF in MDMs (Figure 2G).

211 Other targets of Vpr have been reported. It recruits SLX4-SLX1/MUS81-EME1
212 endonucleases to DCAF1, activating MUS81 degradation and triggering arrest in G2/M (33). It

213 also degrades helicase-like transcription factor (HLTF), a protein recently shown to enhance
214 infection of HIV-1 in T-cell lines (8, 12). To determine if the depletion of REAF requires the
215 association of Vpr with DCAF1, we generated another mutant virus with a different substitution
216 within *vpr*, Q65R. Previously, the Q65R mutation was shown to ablate the association between
217 DCAF1 and Vpr and the ability of Vpr to induce arrest at G2/M (34-36). Figures 2H and I show
218 that this mutant, compared to HIV-1 89.6^{WT}, is unable to down modulate REAF. We cannot rule
219 out inhibition of synthesis or increased nuclear export in addition to degradation as possibilities.
220

221 **Expression of REAF during cell cycle**

222 A phenotype of HIV-1 Vpr is that it can induce cell cycle arrest at G2/M in cycling T cells
223 (27, 37-39). The failure of both HIV-1 89.6^{F34I} and HIV-1 89.6^{Q65R} to efficiently induce G2/M
224 arrest (30, 34, 40-42), and our observation that they cannot down modulate REAF (Figures 2G, H
225 and I), prompted us to investigate REAF and the cell cycle.

226 First, we determined the expression levels of REAF at various phases of the cell cycle using
227 imaging flow cytometry (Figure 3A). REAF protein levels are lowest in G0/1, increase through S
228 phase, and peak in G2/M. Confocal microscopy of cycling cells concurred with the quantitative
229 analysis in Figure 3A, overall REAF levels appeared greater in mitotic cells (Figure 3B). There is
230 also an apparent exclusion of REAF from the nuclear region of the cell during mitosis (particularly
231 during metaphase, anaphase and telophase). Quantitative analysis by imaging flow cytometry of
232 cycling cells confirmed that the mitotic population had a lower nuclear enrichment score (0.13)
233 compared to the non-mitotic cells (1.53), indicating a lower intensity of REAF in the nucleus
234 compared to in the cell as a whole (Figure 3C). Representative images of subcellular REAF in
235 mitotic and non-mitotic cells from imaging flow cytometry are presented in Figure 3D.

236 To determine if the G2/M arrest phenotype, induced by Vpr, could be related to its ability
237 to down modulate REAF, we generated inducible THP-1 and PM1 cell lines that upon induction
238 produce shRNA targeting either REAF or a scrambled control sequence (SCR). After knockdown
239 of REAF in THP-1, there was a clear increase in the expression of the mitotic marker,
240 phosphorylated histone H3 (Ser10/Thr11) (Figure 3E). However, when measured more
241 quantitatively by DNA content analysis in PM1, the potency of the G2/M arrest appeared weak
242 compared to the levels previously described (30, 39). REAF down modulation in PM1 was
243 confirmed by a reduction in mRNA and in protein (Figure 3F and G). Cell cycle phase profiles
244 were determined by flow cytometry (Figure 3H). The increase in the G2/G1 ratio of cells with
245 REAF knocked down, although small (Figure 3H, insert), was comparable to other reports where
246 individual reported targets of Vpr were knocked down (14). In agreement with Greenwood *et al.*
247 2019, we contend that more than one protein may be required to produce the strong Vpr induced
248 G2/M arrest reported (14, 30, 39).
249
250 **REAF is not IFN stimulated or under positive selection.**
251 IFNα is central to innate immune responses and is known to induce many HIV-1 restriction
252 factors (43, 44). We used RNA microarray analysis to determine if IFNα upregulated REAF
253 mRNA in MDMs. Figure 4A shows that IFNα induced upregulation of many known antiviral
254 genes, including HIV restriction factors APOBEC3G, MX2, Tetherin and Viperin (45)(46)(43)
255 but with little or no upregulation of REAF mRNA. Nevertheless, antiviral factors are also often
256 upregulated in response to pathogen associated molecular patterns (PAMPs). Poly(I:C) is a double-
257 stranded RNA, used to stimulate molecular pattern recognition pathways associated with viral
258 infection. Figure 4B shows that poly(I:C) induces REAF in THP-1, a macrophage cell line.

259 Lipopolysaccharide (LPS), another PAMP which is TLR4 specific (47), also induces the
260 upregulation of REAF expression in PBMCs (Figure 4C).

261 Restriction factors are often under evolutionary positive selection at sites that interact with
262 virus. We compared REAF DNA sequences from 15 extant primate species using PAML package
263 for signatures of positive natural selection. We found no evidence of positive selection of REAF
264 in the primate lineage (Figure 4D).

265

266

267

268

269

270

271

272

273

274

275

276

277

278

279

280

281 ## Discussion

282 The deletion of *vpr* in HIV-1 leads to impairment of its replication in both HeLa-CD4 and
283 primary macrophages. A number of experiments presented here point to a role for Vpr in the
284 counter-restriction of the antiviral protein REAF. First, HIV-1 replication is significantly enhanced
285 by knockdown of REAF in either HeLa-CD4 or primary macrophages and this phenotype is more
286 pronounced for viruses lacking *vpr*. Second, REAF is down modulated early after infection in a
287 manner dependent on both the presence of Vpr and, as demonstrated by *vpr* single point mutations,
288 the localization of Vpr to the nuclear envelope and its interaction with a nuclear localised E3
289 ubiquitin ligase, DCAF1. Third, using VLPs we show that Vpr alone is sufficient to down
290 modulate REAF in MDMs. Finally, by co-immunoprecipitation, we demonstrate that REAF and
291 Vpr physically interact, either directly, or indirectly as part of a complex. Taken together, our
292 results highlight the importance of the relationship between REAF and the HIV-1 accessory
293 protein Vpr.

294 Others have shown a specific requirement for Vpr in the efficient infection of non-dividing
295 cells and less so in cycling T cells (12, 27, 30). The requirement for Vpr in macrophage infection
296 is substantiated here, reduced viral replication is observed after infection of MDMs with either
297 HIV-1 $89.6^{\Delta vpr}$ or HIV-1 89.6^{F34I} compared to HIV-1 89.6^{WT}. This is the first demonstration of a
298 *vpr*-alleviated impairment of HIV-1 replication in primary macrophages. Recently Yan *et al.*
299 (2019) show that HLTF, a reported target of Vpr, restricts replication of HIV-1 in T cells while
300 Lahouassa *et al.* (2016) also reported a Vpr dependent loss of HLTF at six hours post infection (8,
301 12). HLTF down modulation occurs concomitantly with REAF as early as 0.5 hours post infection
302 (data not shown). Interestingly, HLTF and REAF were identified in the same screen for proteins
303 that interact with single-stranded DNA (48).

304 The transient nature and timing of REAF depletion shown here is consistent with its ability
305 to impede the production of reverse transcripts early in infection (20). After an initial down
306 modulation of REAF following infection, REAF depletion is paused, perhaps attributable to the
307 limited quantities of Vpr carried in the virus particle (17). Recently, Greenwood *et al.* carried out
308 a whole cell proteomics screen for factors up or down modulated by Vpr in T cells. They identified
309 almost 2000 proteins affected, underlining the promiscuous activity of Vpr (14). In light of these
310 findings, it is important that attention is directed to those reported Vpr targets that affect replication
311 of HIV-1 in primary cells.

312 Our model is that Vpr is carried into the cell by HIV-1, in limited, but sufficient quantities
313 to down modulate REAF in the timeframe required for reverse transcription to proceed unhindered.
314 Interestingly, nuclear localisation of Vpr is also required for the down modulation of REAF,
315 perhaps similar to the Vpx mediated depletion of the reverse transcription inhibitor SAMHD1 (for
316 which degradation is initiated in the nucleus) (49). Localisation of Vpr to the nuclear region is a
317 requirement for interaction with REAF and DCAF1 and this results in the degradation of REAF.
318 We propose that REAF is linked to the innate immune response as treatment of cells with poly(I:C)
319 or LPS induces its expression. Furthermore, HIV-1 replication without an intact *vpr*, induces the
320 expression of REAF to high levels in primary macrophages as early as 30 minutes post infection.

321 A poorly understood event is that Vpr induces cell cycle arrest in the G2/M phase after
322 infection. We report here that the loss of REAF from cycling cells contributes to an accumulation
323 of the population in G2/M. However, the levels of G2/M induction are weak compared to early
324 reports (30, 39). Thus, we contend that Vpr-induced knock down of more than one protein by Vpr
325 may be required for the complete induction of G2/M arrest seen previously. In support of this,
326 G2/M arrest was only weakly induced when Greenwood *et al.* independently knocked down

327 several Vpr targeted proteins such as MCM10, SMN1, CDCA2 and ZNF267 (14).

328 REAF is unlike the evolving HIV restriction factors such as APOBEC3G, SAMHD1,
329 TRIM5 or BST2/Tetherin and is more similar to SERINC3 and 5 which are not under positive
330 selection (50, 51). REAF has many properties of restriction factors (45, 52). It interacts with HIV-
331 1 reverse transcripts, impeding reverse transcription (20). It is germline encoded, constitutively
332 expressed in cells, regulated by the proteasome system, suppressed by an accessory protein, Vpr,
333 and upregulated by poly(I:C) and LPS. Our results support the current model for Vpr activity which
334 is that it induces the degradation of proteins involved in an unknown restriction of HIV-1. We
335 propose that REAF may be a crucial component a Vpr targeted restriction system that is active
336 against HIV-1.

337

338

339

340

341

342

343

344

345

346

347

348 ## Materials and Methods

349 ### Ethics Statement

350 Leucocyte cones, from which PBMCs were isolated, were obtained from the NHS Blood
351 Transfusion service at St. George's Hospital, London. Donors were anonymous and thus patient
352 consent was not required. The local ethical approval reference number is 06/Q0603/59.

353

354 ### Cell Lines

355 HEK-293T (ATCC), PM1, THP-1, C8166, HeLa-CD4 (all NIBSC AIDS Reagents) and
356 HeLa-CD4 shRNA-REAF (previously described) (18) were maintained at 37°C in 5% CO_2. Cells
357 were cultured in Dulbecco's Modified Eagle Medium (DMEM, Thermo Fisher) supplemented
358 with fetal bovine serum (FBS) 5-10% and appropriate antibiotics (all Thermo Fisher). HeLa-CD4-
359 shRNA-REAF were selected for resistance to puromycin in media supplemented with 10µg/ml
360 puromycin (Invitrogen).

361 The isopropyl β-D-1-thiogalactopyranoside (IPTG)-inducible vector pLKO-IPTG-3xLacO
362 (Sigma) was used to express short hairpin RNAs (shRNAs) targeted against REAF (Mission
363 TRCN0000141116, Sigma). Additionally, a non-target (scramble) control was prepared. Viral
364 particles for cell line transductions were prepared by co-transfecting HEK-293T cells with pLKO-
365 IPTG-3xLacO, the Gag/Pol packaging vector pLP1, a Rev expression vector pLP2, and the
366 vesicular stomatitis virus G protein (VSV-G) expression vector pVPack-VSV-G (Stratagene).
367 After 72 hours, virus was clarified by low-speed centrifugation and passed through a 0.45-m-pore-
368 size filter. THP-1 and PM1 cells were transduced by culturing viral particles in the presence of
369 8g/ml Polybrene for 72 hours, after which resistant colonies were selected and maintained with
370 2µg/ml puromycin. Culturing cells in the presence of 1mM IPTG for 72 hours induced expression

371 of shRNAs.

372

373 **Transfections and Virus/VLP Production**

374 The infectious molecular clone for HIV-1 89.6 was obtained from the Centre for AIDS
375 Research (NIBSC, UK). Infectious full-length and chimeric HIV clones were prepared by linear
376 polyethylenimine 25K (Polysciences), Lipofectamine 2000 (Invitrogen) or Lipofectamine 3000
377 (Invitrogen) transfection of HEK-293T. Virus-like particles (VLPs) were produced by linear
378 polyethylenimine 25K (Polysciences) transfection of HEK-293T. The VLP packaging vector was
379 a gift from N. Landau and production is described in reference (27).

380 The plasmid construct HIV-1 $89.6^{\Delta vpr}$ was generated from the HIV-1 89.6 molecular clone,
381 using overlap extension PCR *(44)*. Clones were confirmed by plasmid sequencing (Source
382 BioScience). Primer sequences are available upon request. HIV-1 p89.6 *vpr* mutants F34I and
383 Q65R were made by site directed mutagenesis (Agilent) of the p89.6 plasmid. HEK-293T were
384 plated at $2x10^4/cm^2$ in 10cm dishes (for virus and VLP production) 48 hours prior to transfection.
385 For virus/VLP production, supernatant was harvested 72 hours post transfection and cleared of cell
386 debris by centrifugation at 500 x *g* for 5 minutes. All viruses were amplified by C8166 for 48 hours
387 prior to harvest.

388

389 **Titration of Replication Competent Virus**

390 HeLa-CD4 were seeded at 1.5×10^4 cells/well in 48-well plates to form an adherent
391 monolayer of cells. Cell monolayers were challenged with serial 1/5 dilutions of virus and titre
392 was assessed after 48 hours by *in situ* intracellular staining of HIV-1 p24 to identify individual
393 foci of viral replication (FFU), as described previously (53). For infection time course experiments,

394 400-500µl of 1×10^5 FFU/ml (HeLa-CD4) or 3×10^3 FFU/ml (MDMs) virus was added per well to
395 cells cultured in 6-well trays for 24 hours (HeLa-CD4) or 7 days (for MDMs). For Figure 2F and
396 2H, cells were challenged with 50ng p24 in 6-well plates with 2×10^6 MDMs per well. For Figure
397 2F, supernatants were harvested on days 0, 2, 8, 21 and 28 post challenge and p24 concentration
398 analysed by ELISA.
399
400 **p24 ELISA**
401 ELISA plates were pre-coated with 5µg/ml sheep anti-HIV-1 p24 antibody (Aalto Bio
402 Reagents) at 4°C overnight. Viral supernatants were treated with 1% Empigen® BB for 30 minutes
403 at 56°C, then plated at 1:10 dilution in tris-bufered saline (TBS) on pre-coated plates and incubated
404 for 3 hours at room temperature. Alkaline phosphatase-conjugated mouse anti-HIV-1 p24
405 monoclonal antibody (Aalto Bio Reagents) in TBS 20% sheep serum, 0.05% v/v Tween-20 was
406 then added and incubated for 1 hour at room temperature. After 4 washes with PBS 0.01% v/v
407 Tween-20 and 2 washes with ELISA Light washing buffer (ThermoFisher), CSPD substrate with
408 Sapphire II enhancer (ThermoFisher) was added and incubated for 30 minutes at room temperature
409 before chemiluminescence detection using a a plate reader.
410
411 **cDNA Synthesis and qPCR**
412 Total RNA was extracted from PM1 cells using the ReliaPrep RNA Kit (Promega). One-
413 step reverse transcription qPCR (Quantbio) using TaqMan probes detected amplified transcripts.
414 Data acquired by an Agilent Mx3000 was analyzed with MxPro software.
415
416 **Gene Expression RNA microarray**

417 Prior to microarray analysis, RNA from MDMs was prepared using the Illumina™
418 TotalPrep™ RNA Amplification Kit (Ambion), according to manufacturer's instructions. The
419 probes were hybridized on an Illumina™ HT12v3 bead array following the manufacturer's standard
420 hybridization and scanning protocols. Raw measurements were processed by GenomeStudio
421 software (Illumina), and quantile normalized. Microarray data are publicly available in the Gene
422 Expression Omnibus (GEO) database with accession number GSE54455.

423

424 **IFN, Poly(I:C) and LPS Treatment**

425 MDMs were treated with IFN (500IU/ml) for 24 hours before harvest for RNA extraction.
426 Recombinant IFNα was purchased from Sigma (Interferon-αA/D human Cat. No. I4401-100KU)
427 and is a combination of human subtypes 1 and 2. THP-1 were treated with poly(I:C) (25μg/ml,
428 HMW/LyoVec™, Invitrogen) for 48 hours before analysis by Western blotting. Prior to poly(I:C)
429 treatment, THP-1 were treated with phorbol 12-myristate 13-acetate (PMA, 62ng/ml) for 3 days
430 and then PMA-free DMEM for 2 days to allow differentiation and recovery. PBMCs isolated from
431 healthy blood donors were treated with lipopolysaccharide (LPS, 10 ng/ml) for 24 hours before
432 analysis by Western blotting.

433

434 **Western blotting**

435 Cells were harvested and lysed in 30-50μl of radioimmunoprecipitation assay (RIPA)
436 buffer supplemented with NaF (5μM), Na_2VO_3 (5μM), β-glycerophosphate (5μM) and 1x Protease
437 Inhibitor Cocktail (Cytoskeleton). The protein concentration of each sample was determined using
438 BCA Protein Assay Kit (Pierce). 12.5-70μg of total protein was separated by SDS-PAGE (4-12%
439 Bis-Tris Gels, Invitrogen), at 120V for 1 hour 45 minutes in MOPS SDS Running Buffer

440 (Invitrogen). Separated proteins were transferred onto nitrocellulose membrane (0.45μm pore size,
441 GE Healthcare) at 45V for 2 hours, in ice-cold 20% (v/v) Methanol NuPAGE™ Transfer Buffer
442 (ThermoFisher). After transfer, membranes were stained for total protein using Ponceau S staining
443 solution (0.1% (w/v) Ponceau in 5% (v/v) acetic acid), washed 3 times for 5 minutes on an orbital
444 shaker in dH_2O and imaged using ChemiDoc Gel Imaging System. Membranes were blocked for
445 1 hour at room temperature in 5% (w/v) non-fat milk powder in TBS-T buffer. Specific proteins
446 were detected with primary antibodies by incubation with membranes overnight at 4^oC and with
447 secondary antibodies for 1 hour at room temperature. All antibodies were diluted in blocking
448 buffer. Proteins were visualized using ECL Prime Western Blotting Detection Reagent (GE
449 Healthcare) and imaged using either ChemiDoc Gel Imaging System (Bio-Rad) or exposed to CL-
450 XPosure films (ThermoScientific) and developed. In all places where quantitative comparisons are
451 made, such as in Figures 1D and E, blots are derived from the same blot or blots processed together.
452

453 **Antibodies**

454 Primary rabbit polyclonal antibody to REAF (RbpAb-RPRD2) has been previously
455 described (20). For imaging flow cytometry and confocal microscopy, RbpAb-RPRD2 was
456 detected using goat anti-rabbit IgG conjugated with Alexa Fluor 647 (Invitrogen). FITC-labelled
457 anti-phospho-histone H3 (Ser28) Alexa 488 was used (BD Bioscience) for imaging flow cytometry
458 and confocal microscopy. MsmAb-GFP (both Abcam) was detected by anti-mouse IgG antibody
459 conjugated to HRP (GE Healthcare) for Western blotting. Also for Western blotting, RbpAb-
460 RPRD2, RbmAb-IFITM3 (EPR5242, Insight Biotechnology), RbpAb-GAPDH, and RbmAb-
461 phospho-histone H3 (Ser10/Thr11) were detected with donkey anti-rabbit IgG conjugated to HRP
462 (GE Healthcare).

463

464 **Immunoprecipitation**

465 HEK-293T, transfected with either Vpr-GFP expression plasmid or GFP control
466 expression vector, were lysed 72hrs post transfection in RIPA buffer supplemented with NaF
467 (5μM), Na_2VO_3 (5μM), β-glycerophosphate (5μM) and 1x Protease Inhibitor Cocktail
468 (Cytoskeleton). Total protein concentration was determined using BCA Protein Assay Kit (Pierce).
469 GFP-TRAP® magnetic agarose beads were equilibrated in ice cold dilution buffer (10 mM Tris/Cl
470 pH 7.5; 150 mM NaCl; 0.5 mM EDTA) according to manufacturer's instructions (Chromotek).
471 Cell lysates containing 100μg of total protein were incubated with 10μl of equilibrated beads for
472 2 hours at 4°C with gentle agitation. Beads were washed three times with PBST buffer before
473 analysis of immunoprecipitated protein by Western blotting.

474

475 **Magnetic Separation of Primary Human Lymphocytes**

476 Peripheral blood mononuclear cells (PBMCs) were isolated from leukocyte cones (NHS
477 Blood Transfusion service, St. George's Hospital, London) by density gradient centrifugation with
478 Lymphoprep™ density gradient medium (STEMCELL™ Technologies). Peripheral monocytes
479 were isolated from PBMCs, using the human $CD14^+$ magnetic beads (Miltenyi Biotech) according
480 to manufacturer's instructions. $CD4^+$ T cells were isolated from the flow-through, using the human
481 $CD4^+$ T cell isolation kit (Miltenyi Biotech). $CD14^+$ monocytes, and $CD4^+$ T cells were either
482 differentiated, or fixed directly after isolation for intracellular staining. To obtain M1 and M2
483 macrophages (M1/M2 MDMs), monocytes were treated with either granulocyte-macrophage
484 colony stimulating factor (GM-CSF, 100ng/ml, Peprotech) or macrophage colony stimulating
485 factor (M-CSF, 100ng/ml) for 7 days, with medium replenished on day 4. To obtain dendritic cells

486 (DC), monocytes were treated with GM-CSF (50ng/ml) and IL-4 (50ng/ml) for 7 days, with
487 medium replenished on day 4. Activated $CD4^+$ T cells were obtained by stimulating freshly
488 isolated $CD4^+$ T cells at $1x10^6$/ml with T cell activator CD3/CD28 Dynabeads (ThermoFisher), at
489 a bead-cell-ratio of 1, for 7 days. Magnetic beads were removed prior to intracellular staining and
490 imaging flow cytometry.

491

492 **Immunofluorescence**

493 HeLa-CD4 were plated at $2x10^4/cm^2$ in 8-well chamber slides for confocal microscopy.
494 Cells were washed with PBS, fixed in 2% paraformaldehyde/PBS for 10 minutes at room
495 temperature. Fixed cells were permeabilized in 0.2% Triton™-X100/PBS for 20 minutes at room
496 temperature and incubated with primary antibodies in PBS 0.1% Triton-X100 2% BSA overnight
497 at 4^0C. After 3 washes in PBS, cells were labelled with secondary antibodies in the same buffer
498 for 1 hour at room temperature, and washed 3 times with PBS. Nuclei were counterstained with
499 Hoechst 33342 (2µM, ThermoFisher) for 5 minutes at room temperature. Labelled cells were
500 mounted with ProLong™ Diamond Antifade Mountant (ThermoFisher) and analyzed on a laser
501 scanning confocal microscope LSM 710 (Carl Zeiss). Images were acquired with ZEN software
502 and analyzed with ImageJ.

503

504 **Imaging Flow Cytometry**

505 Cells were fixed in FIX&PERM® Solution A (Nordic MUbio) for 30 minutes, and
506 permeabilized with 0.2% Triton™-X 100/PBS. MDMs were blocked with human serum (1%). The
507 staining buffer used was: 0.1% Triton™-X 100 0.5% FBS. Nuclei were counterstained with DAPI
508 (1µg/ml) for two hours. Imaging flow cytometry was performed using the Amnis ImageStream®x

509 Mark II Flow Cytometer (Merck) and INSPIRE® software (Amnis). A minimum of 5000 events
510 were collected for each sample. IDEAS® software (Amnis) was used for analysis and to determine
511 the 'nuclear enrichment score' (NES). The NES is a comparison of the intensity of REAF
512 fluorescence inside the nucleus (defined using the exclusively nuclear stain DAPI) to the total
513 fluorescence intensity of REAF in the entire cell (defined using brightfield images). A lower
514 nuclear enrichment score indicates a lower proportion of overall REAF is located within the
515 nucleus.
516

517 **Statistics**

518 Statistical significance in all experiments was calculated by Student's t-test (two tailed) or
519 ANOVA (indicated). Data are represented as mean ± standard deviation (error bars). GraphPad
520 Prism and Excel were used for calculation and illustration of graphs.
521

522 **Cell Cycle Analysis**

523 Cell cycle phase distribution was determined by analysis of DNA content via either flow
524 cytometry (BD FACS Canto™ II) or imaging flow cytometry. Cells were fixed in FIX&PERM®
525 Solution A (Nordic MUbio) and stained with DAPI (1µg/ml) before analysis by imaging flow
526 cytometry. Cell lysates were assessed by Western blotting using the anti-phospho-histone H3
527 (Ser10/Thr11) antibody as an additional mitotic marker. Chromatin morphology and anti-phospho-
528 histone H3 (Ser28) were used to determine the cells in indicated phases of the cell cycle and mitosis
529 in confocal microscopy experiments. Cell cycle status of PM1 cells was determined via propidium
530 iodide (PI) staining using FxCycle PI/RNse solution (ThermoFisher). Stained cells were analyzed
531 on an NxT flow cytometer (ThermoFisher).

532

533 **Evolutionary Analysis**

534 To ascertain the evolutionary trajectory of REAF, we analyzed DNA sequence alignments
535 of REAF from 15 species of extant primates using codeml (as implemented by PAML 4.2) (54).
536 The evolution of REAF was compared to several NSsites models of selection, M1, M7 and M8a
537 (neutral models with site classes of dN/dS <1 or ≤1) and M2, M8 (positive selection models
538 allowing an additional site class with dN/dS >1). Two models of codon frequencies (F61 and F3x4)
539 and two different seed values for dN/dS (ω) were used in the maximum likelihood simulations.
540 Likelihood ratio tests were performed to evaluate which model of evolution the data fit
541 significantly better. The p-value indicates the confidence with which the null model (M1, M7,
542 M8a) can be rejected in favor of the model of positive selection (M2, M8). The alignment of REAF
543 was analyzed by GARD to confirm the lack recombination during REAF evolution (55). Neither
544 positively selected sites nor signatures of episodic diversifying selection were detected within
545 REAF by additional evolutionary analysis by REL and FEL or MEME (56).

546

547 **Data Availability**

548 All RNA microarray data is available in the gene expression omnibus (GEO) database with
549 accession number GSE54455.

550

551

552

553

554

Acknowledgements: This work was supported partly by an MRC Senior Non-Clinical Fellowship awarded to AM (G117/547) and PhD studentships awarded by QMUL Life Sciences Institute (LSI) (CEJ) and The Rosetrees Trust (JMG and CEJ, M665 and M275). RDS was supported by the Wellcome Trust-University of Edinburgh Institutional Strategic Support Fund. The monoclonal antibodies to HIV-1 p24 (EVA365 and 366) were provided by the EU Programme EVA Centre for AIDS Reagents, NIBSC, UK (AVIP Contract Number LSHP-CT-2004-503487). The Wellcome Trust (101604/Z/13/Z) funded the purchase of Amnis ImageStream™ imaging flow cytometer. We wish to thank N. Landau for the kind gift of VPL constructs.

577 **References:**

578

579 1. **Eckstein DA, Sherman MP, Penn ML, Chin PS, De Noronha CM, Greene WC,**
580 **Goldsmith MA.** 2001. HIV-1 Vpr enhances viral burden by facilitating infection of
581 tissue macrophages but not nondividing CD4+ T cells. J Exp Med **194:**1407-1419.
582 2. **Malim MH, Emerman M.** 2008. HIV-1 accessory proteins--ensuring viral survival in a
583 hostile environment. Cell Host Microbe **3:**388-398.
584 3. **Zhou X, DeLucia M, Ahn J.** 2016. SLX4-SLX1 Protein-independent Down-regulation
585 of MUS81-EME1 Protein by HIV-1 Viral Protein R (Vpr). J Biol Chem **291:**16936-
586 16947.
587 4. **Schrofelbauer B, Yu Q, Zeitlin SG, Landau NR.** 2005. Human immunodeficiency
588 virus type 1 Vpr induces the degradation of the UNG and SMUG uracil-DNA
589 glycosylases. J Virol **79:**10978-10987.
590 5. **Romani B, Shaykh Baygloo N, Aghasadeghi MR, Allahbakhshi E.** 2015. HIV-1 Vpr
591 Protein Enhances Proteasomal Degradation of MCM10 DNA Replication Factor through
592 the Cul4-DDB1[VprBP] E3 Ubiquitin Ligase to Induce G2/M Cell Cycle Arrest. J Biol
593 Chem **290:**17380-17389.
594 6. **Maudet C, Sourisce A, Dragin L, Lahouassa H, Rain JC, Bouaziz S.** 2013. HIV-1
595 Vpr induces the degradation of ZIP and sZIP, adaptors of the NuRD chromatin
596 remodeling complex, by hijacking DCAF1/VprBP. PLoS ONE **8**.
597 7. **Lv L, Wang Q, Xu Y, Tsao LC, Nakagawa T, Guo H, Su L, Xiong Y.** 2018. Vpr
598 Targets TET2 for Degradation by CRL4(VprBP) E3 Ligase to Sustain IL-6 Expression
599 and Enhance HIV-1 Replication. Mol Cell **70:**961-970 e965.
600 8. **Lahouassa H, Blondot ML, Chauveau L, Chougui G, Morel M, Leduc M.** 2016.
601 HIV-1 Vpr degrades the HLTF DNA translocase in T cells and macrophages. Proc Natl
602 Acad Sci USA **113**.
603 9. **Laguette N, Brégnard C, Hue P, Basbous J, Yatim A, Larroque M.** 2014. Premature
604 activation of the SLX4 complex by Vpr promotes G2/M arrest and escape from innate
605 immune sensing. Cell **156**.
606 10. **Hrecka K, Hao C, Shun MC, Kaur S, Swanson SK, Florens L, Washburn MP,**
607 **Skowronski J.** 2016. HIV-1 and HIV-2 exhibit divergent interactions with HLTF and
608 UNG2 DNA repair proteins. Proc Natl Acad Sci U S A **113:**E3921-3930.
609 11. **Hofmann S, Dehn S, Businger R, Bolduan S, Schneider M, Debyser Z, Brack-**
610 **Werner R, Schindler M.** 2017. Dual role of the chromatin-binding factor PHF13 in the
611 pre- and post-integration phases of HIV-1 replication. Open Biol **7**.
612 12. **Yan J, Shun MC, Zhang Y, Hao C, Skowronski J.** 2019. HIV-1 Vpr counteracts
613 HLTF-mediated restriction of HIV-1 infection in T cells. Proc Natl Acad Sci U S A
614 **116:**9568-9577.
615 13. **Lahouassa H, Blondot ML, Chauveau L, Chougui G, Morel M, Leduc M,**
616 **Guillonneau F, Ramirez BC, Schwartz O, Margottin-Goguet F.** 2016. HIV-1 Vpr
617 degrades the HLTF DNA translocase in T cells and macrophages. Proc Natl Acad Sci U
618 S A **113:**5311-5316.
619 14. **Greenwood EJD, Williamson JC, Sienkiewicz A, Naamati A, Matheson NJ, Lehner**
620 **PJ.** 2019. Promiscuous Targeting of Cellular Proteins by Vpr Drives Systems-Level
621 Proteomic Remodeling in HIV-1 Infection. Cell Rep **27:**1579-1596 e1577.

622 15. **Cohen EA, Terwilliger EF, Jalinoos Y, Proulx J, Sodroski JG, Haseltine WA.** 1990.
623 Identification of HIV-1 vpr product and function. J Acquir Immune Defic Syndr **3:**11-18.
624 16. **Bachand F, Yao XJ, Hrimech M, Rougeau N, Cohen EA.** 1999. Incorporation of Vpr
625 into human immunodeficiency virus type 1 requires a direct interaction with the p6
626 domain of the p55 gag precursor. J Biol Chem **274:**9083-9091.
627 17. **Desai TM, Marin M, Sood C, Shi J, Nawaz F, Aiken C, Melikyan GB.** 2015.
628 Fluorescent protein-tagged Vpr dissociates from HIV-1 core after viral fusion and rapidly
629 enters the cell nucleus. Retrovirology **12:**88.
630 18. **Marno KM, O'Sullivan E, Jones CE, Diaz-Delfin J, Pardieu C, Sloan RD, McKnight**
631 **A.** 2017. RNA-Associated Early-Stage Antiviral Factor Is a Major Component of Lv2
632 Restriction. J Virol **91**.
633 19. **McKnight A, Griffiths DJ, Dittmar M, Clapham P, Thomas E.** 2001. Characterization
634 of a late entry event in the replication cycle of human immunodeficiency virus type 2. J
635 Virol **75**.
636 20. **Marno KM, Ogunkolade BW, Pade C, Oliveira NM, O'Sullivan E, McKnight A.**
637 2014. Novel restriction factor RNA-associated early-stage anti-viral factor (REAF)
638 inhibits human and simian immunodeficiency viruses. Retrovirology **11:**3.
639 21. **Harrison IP, McKnight A.** 2011. Cellular entry via an actin and clathrin-dependent
640 route is required for Lv2 restriction of HIV-2. Virology **415:**47-55.
641 22. **Marchant D, Neil SJ, Aubin K, Schmitz C, McKnight A.** 2005. An envelope-
642 determined, pH-independent endocytic route of viral entry determines the susceptibility
643 of human immunodeficiency virus type 1 (HIV-1) and HIV-2 to Lv2 restriction. J Virol
644 **79:**9410-9418.
645 23. **Reuter S, Kaumanns P, Buschhorn SB, Dittmar MT.** 2005. Role of HIV-2 envelope in
646 Lv2-mediated restriction. Virology **332:**347-358.
647 24. **Schmitz C, Marchant D, Neil SJ, Aubin K, Reuter S, Dittmar MT, McKnight A.**
648 2004. Lv2, a novel postentry restriction, is mediated by both capsid and envelope. J Virol
649 **78:**2006-2016.
650 25. **Zuba-Surma EK, Kucia M, Abdel-Latif A, Lillard JW, Jr., Ratajczak MZ.** 2007.
651 The ImageStream System: a key step to a new era in imaging. Folia Histochem Cytobiol
652 **45:**279-290.
653 26. **Han Y, Gu Y, Zhang AC, Lo YH.** 2016. Review: imaging technologies for flow
654 cytometry. Lab Chip **16:**4639-4647.
655 27. **Connor RI, Chen BK, Choe S, Landau NR.** 1995. Vpr is required for efficient
656 replication of human immunodeficiency virus type-1 in mononuclear phagocytes.
657 Virology **206**.
658 28. **Connor RI, Chen BK, Choe S, Landau NR.** 1995. Vpr is required for efficient
659 replication of human immunodeficiency virus type-1 in mononuclear phagocytes.
660 Virology **206:**935-944.
661 29. **Heinzinger NK, Bukrinsky MI, Haggerty SA, Ragland AM, Kewalramani V, Lee**
662 **MA, Gendelman HE, Ratner L, Stevenson M, Emerman M.** 1994. The Vpr protein of
663 human immunodeficiency virus type 1 influences nuclear localization of viral nucleic
664 acids in nondividing host cells. Proc Natl Acad Sci U S A **91:**7311-7315.
665 30. **Vodicka MA, Koepp DM, Silver PA, Emerman M.** 1998. HIV-1 Vpr interacts with the
666 nuclear transport pathway to promote macrophage infection. Genes Dev **12:**175-185.

667 31. **Balliet JW, Kolson DL, Eiger G, Kim FM, McGann KA, Srinivasan A.** 1994. Distinct
668 effects in primary macrophages and lymphocytes of the human immunodeficiency virus
669 type 1 accessory genes vpr, vpu, and nef: mutational analysis of a primary HIV-1 isolate.
670 Virology **200**.
671 32. **Chen R, Le Rouzic E, Kearney JA, Mansky LM, Benichou S.** 2004. Vpr-mediated
672 incorporation of UNG2 into HIV-1 particles is required to modulate the virus mutation
673 rate and for replication in macrophages. J Biol Chem **279:**28419-28425.
674 33. **Laguette N, Bregnard C, Hue P, Basbous J, Yatim A, Larroque M, Kirchhoff F,**
675 **Constantinou A, Sobhian B, Benkirane M.** 2014. Premature activation of the SLX4
676 complex by Vpr promotes G2/M arrest and escape from innate immune sensing. Cell
677 **156:**134-145.
678 34. **Jacquot G, Le Rouzic E, Maidou-Peindara P, Maizy M, Lefrere JJ, Daneluzzi V,**
679 **Monteiro-Filho CM, Hong D, Planelles V, Morand-Joubert L, Benichou S.** 2009.
680 Characterization of the molecular determinants of primary HIV-1 Vpr proteins: impact of
681 the Q65R and R77Q substitutions on Vpr functions. PLoS One **4:**e7514.
682 35. **Le Rouzic E, Belaidouni N, Estrabaud E, Morel M, Rain JC, Transy C, Margottin-**
683 **Goguet F.** 2007. HIV1 Vpr arrests the cell cycle by recruiting DCAF1/VprBP, a receptor
684 of the Cul4-DDB1 ubiquitin ligase. Cell Cycle **6:**182-188.
685 36. **Le Rouzic E, Morel M, Ayinde D, Belaidouni N, Letienne J, Transy C, Margottin-**
686 **Goguet F.** 2008. Assembly with the Cul4A-DDB1DCAF1 ubiquitin ligase protects HIV-
687 1 Vpr from proteasomal degradation. J Biol Chem **283:**21686-21692.
688 37. **He J, Choe S, Walker R, Di Marzio P, Morgan DO, Landau NR.** 1995. Human
689 immunodeficiency virus type 1 viral protein R (Vpr) arrests cells in the G2 phase of the
690 cell cycle by inhibiting p34cdc2 activity. J Virol **69:**6705-6711.
691 38. **Rogel ME, Wu LI, Emerman M.** 1995. The human immunodeficiency virus type 1 vpr
692 gene prevents cell proliferation during chronic infection. J Virol **69:**882-888.
693 39. **Jowett JB, Planelles V, Poon B, Shah NP, Chen ML, Chen IS.** 1995. The human
694 immunodeficiency virus type 1 vpr gene arrests infected T cells in the G2 + M phase of
695 the cell cycle. J Virol **69:**6304-6313.
696 40. **Jacquot G, Le Rouzic E, David A, Mazzolini J, Bouchet J, Bouaziz S, Niedergang F,**
697 **Pancino G, Benichou S.** 2007. Localization of HIV-1 Vpr to the nuclear envelope:
698 impact on Vpr functions and virus replication in macrophages. Retrovirology **4:**84.
699 41. **DeHart JL, Zimmerman ES, Ardon O, Monteiro-Filho CM, Argañaraz ER,**
700 **Planelles V.** 2007. HIV-1 Vpr activates the G2 checkpoint through manipulation of the
701 ubiquitin proteasome system. Virol J **4**.
702 42. **Maudet C, Bertrand M, Le Rouzic E, Lahouassa H, Ayinde D, Nisole S, Goujon C,**
703 **Cimarelli A, Margottin-Goguet F, Transy C.** 2011. Molecular insight into how HIV-1
704 Vpr protein impairs cell growth through two genetically distinct pathways. J Biol Chem
705 **286:**23742-23752.
706 43. **Goujon C, Malim MH.** 2010. Characterization of the alpha interferon-induced postentry
707 block to HIV-1 infection in primary human macrophages and T cells. J Virol **84:**9254-
708 9266.
709 44. **Cheney KM, McKnight A.** 2010. Interferon-alpha mediates restriction of human
710 immunodeficiency virus type-1 replication in primary human macrophages at an early
711 stage of replication. PLoS One **5:**e13521.

712 45. **Doyle T, Goujon C, Malim MH.** 2015. HIV-1 and interferons: who's interfering with
713 whom? Nat Rev Microbiol **13:**403-413.
714 46. **Malim MH, Bieniasz PD.** 2012. HIV Restriction Factors and Mechanisms of Evasion.
715 Cold Spring Harb Perspect Med **2:**a006940.
716 47. **Hoshino K, Takeuchi O, Kawai T, Sanjo H, Ogawa T, Takeda Y, Takeda K, Akira**
717 **S.** 1999. Cutting edge: Toll-like receptor 4 (TLR4)-deficient mice are hyporesponsive to
718 lipopolysaccharide: evidence for TLR4 as the Lps gene product. J Immunol **162:**3749-
719 3752.
720 48. **Marechal A, Li JM, Ji XY, Wu CS, Yazinski SA, Nguyen HD, Liu S, Jimenez AE,**
721 **Jin J, Zou L.** 2014. PRP19 transforms into a sensor of RPA-ssDNA after DNA damage
722 and drives ATR activation via a ubiquitin-mediated circuitry. Mol Cell **53:**235-246.
723 49. **Brandariz-Nunez A, Valle-Casuso JC, White TE, Laguette N, Benkirane M,**
724 **Brojatsch J, Diaz-Griffero F.** 2012. Role of SAMHD1 nuclear localization in restriction
725 of HIV-1 and SIVmac. Retrovirology **9:**49.
726 50. **McLaren PJ, Gawanbacht A, Pyndiah N, Krapp C, Hotter D, Kluge SF, Gotz N,**
727 **Heilmann J, Mack K, Sauter D, Thompson D, Perreaud J, Rausell A, Munoz M,**
728 **Ciuffi A, Kirchhoff F, Telenti A.** 2015. Identification of potential HIV restriction
729 factors by combining evolutionary genomic signatures with functional analyses.
730 Retrovirology **12:**41.
731 51. **Murrell B, Vollbrecht T, Guatelli J, Wertheim JO.** 2016. The Evolutionary Histories
732 of Antiretroviral Proteins SERINC3 and SERINC5 Do Not Support an Evolutionary
733 Arms Race in Primates. J Virol **90:**8085-8089.
734 52. **Kluge SF, Sauter D, Kirchhoff F.** 2015. SnapShot: antiviral restriction factors. Cell
735 **163:**774-774 e771.
736 53. **McKnight A, Clapham PR, Weiss RA.** 1994. HIV-2 and SIV infection of nonprimate
737 cell lines expressing human CD4: restrictions to replication at distinct stages. Virology
738 **201:**8-18.
739 54. **Yang Z.** 2007. PAML 4: phylogenetic analysis by maximum likelihood. Mol Biol Evol
740 **24:**1586-1591.
741 55. **Kosakovsky Pond SL, Posada D, Gravenor MB, Woelk CH, Frost SD.** 2006. GARD:
742 a genetic algorithm for recombination detection. Bioinformatics **22:**3096-3098.
743 56. **Pond SL, Frost SD.** 2005. Datamonkey: rapid detection of selective pressure on
744 individual sites of codon alignments. Bioinformatics **21:**2531-2533.

745

746

747

748

749

750

751

752

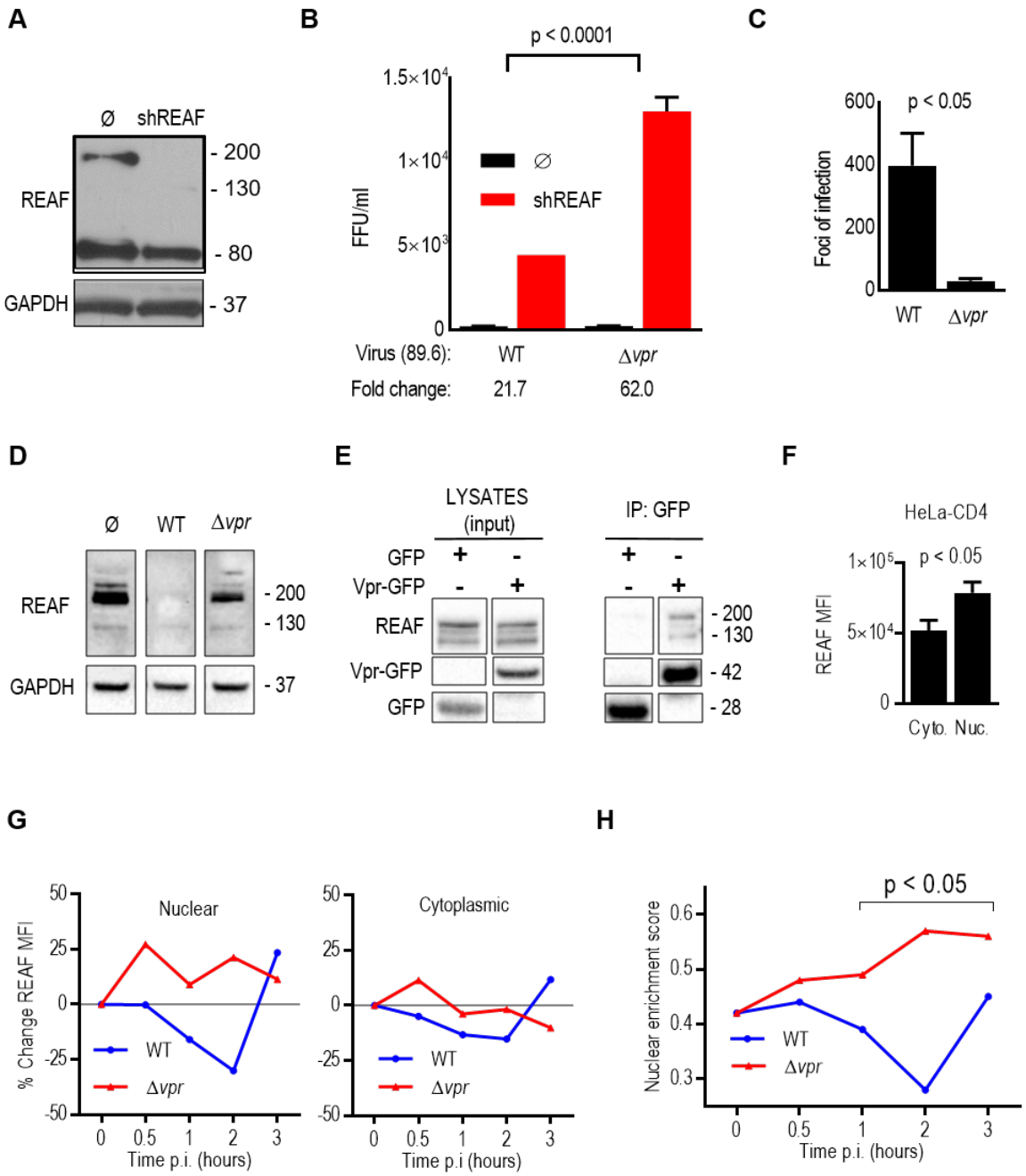

753

754

755

756

757

758 **Figure 1: HIV-1 Vpr interacts with REAF and overcomes restriction. (A)** REAF protein in
759 HeLa-CD4 (Ø) and HeLa-CD4 shRNA-REAF (shREAF). GAPDH is a loading control. **(B)**
760 Infectivity (FFU/ml) of HIV-1 89.6^{WT} and HIV-1 $89.6^{\Delta vpr}$ in HeLa-CD4 (Ø) and HeLa-CD4
761 shRNA-REAF (shREAF). Viral inputs were equivalent at approximately 50 FFU/ml measured on
762 HeLa-CD4. Error bars in indicate the standard deviations of means derived from a range of
763 duplicate titrations. Fold changes in FFU are indicated. **(C)** Resulting foci of infection from equal
764 p24 inputs (1ng) of HIV-1 89.6^{WT} or HIV-1 $89.6^{\Delta vpr}$ in HeLa-CD4. Error bars in indicate the
765 standard deviations of means derived from a range of duplicate titrations. **(D)** REAF protein in
766 Hela-CD4 24 hours post challenge with HIV-1 89.6^{WT} or HIV-1 $89.6^{\Delta vpr}$. GAPDH is a loading
767 control. **(E)** HEK-293T cells were transfected with Vpr-GFP expression plasmid or GFP control
768 vector, expression was analysed by Western blotting (left) and protein was immunoprecipitated
769 (IP) with anti-GFP beads. Co-immunoprecipitated REAF was detected in the Vpr-GFP
770 precipitation (right). **(F)** Nuclear and cytoplasmic REAF mean fluorescence intensity (MFI) in
771 HeLa-CD4 measured by imaging flow cytometry. Error bars represent standard deviations of
772 means of replicates. **(G)** Percentage (%) change in REAF MFI from time '0' in the nucleus (left)
773 and cytoplasm (right) of Hela-CD4 over time after challenge with HIV-1 89.6^{WT} or HIV-1 $89.6^{\Delta vpr}$.
774 Results are representative of three independent experiments. **(H)** Nuclear enrichment score of
775 HeLa-CD4 over time post challenge with HIV-1 89.6^{WT} or HIV-1 $89.6^{\Delta vpr}$. A lower nuclear
776 enrichment score indicates a lower proportion of overall REAF is located in the nucleus as
777 calculated by IDEAS software. Results are representative of three independent experiments.
778 Where quantitative comparisons are made, blots are derived from the same blot or blots processed
779 together.
780

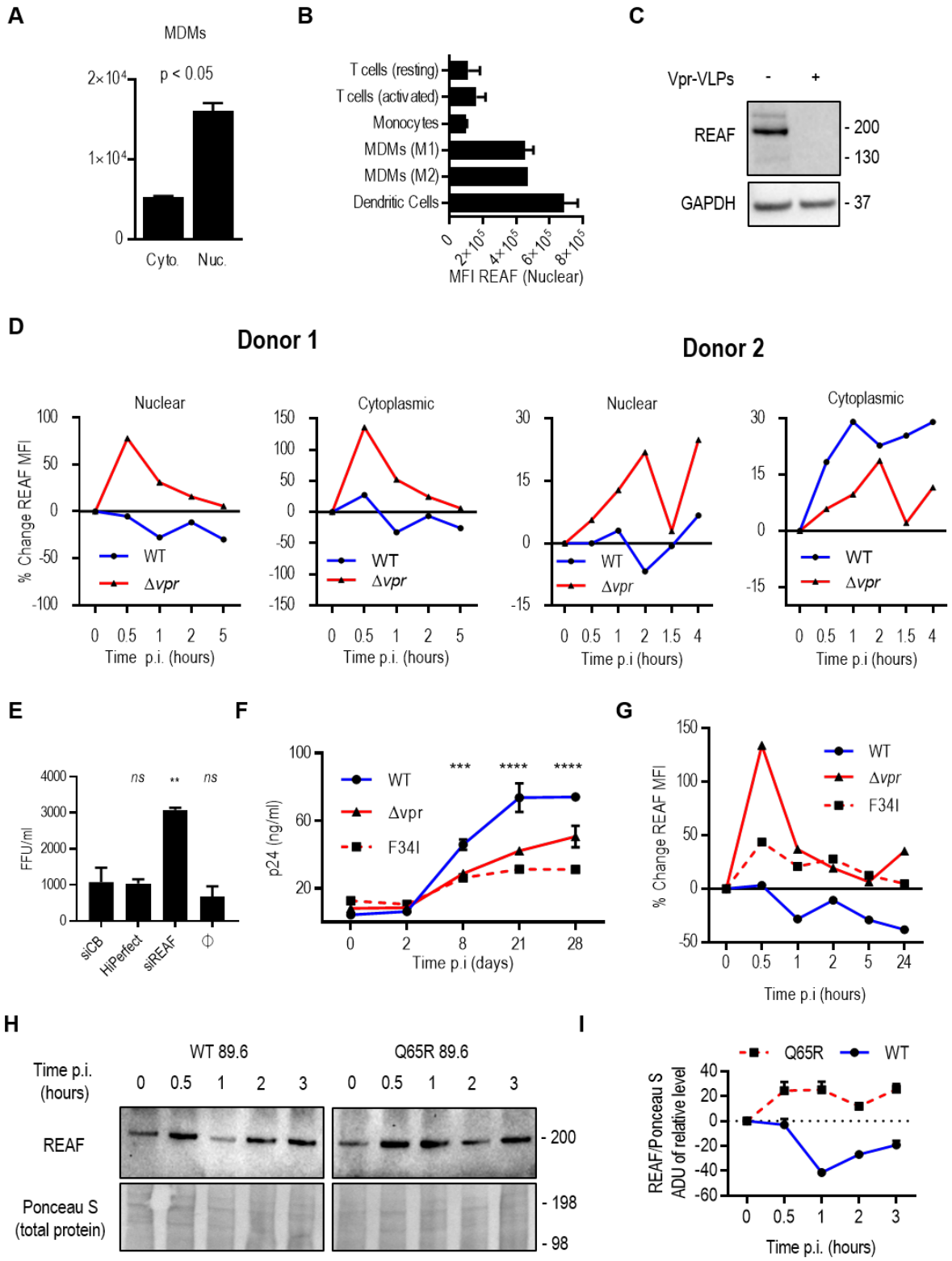
A
MDMs
p < 0.05
2×10⁴
1×10⁴
0
Cyto.
Nuc.
B
T cells (resting)
T cells (activated)
Monocytes
MDMs (M1)
MDMs (M2)
Dendritic Cells
0
2×10⁵
4×10⁵
6×10⁵
8×10⁵
MFI REAF (Nuclear)
C
Vpr-VLPs
-
+
REAF
GAPDH
- 200
- 130
- 37
D
Donor 1
Donor 2
Nuclear
Cytoplasmic
% Change REAF MFI
WT
Δvpr
Time p.i. (hours)
Time p.i (hours)
E
FFU/ml
ns
**
ns
siCB
HiPerfect
siREAF
Φ
F
p24 (ng/ml)
WT
Δvpr
F34I
***
****
****
Time p.i (days)
G
% Change REAF MFI
WT
Δvpr
F34I
Time p.i (hours)
H
WT 89.6
Q65R 89.6
Time p.i. (hours)
REAF
Ponceau S (total protein)
- 200
- 198
- 98
I
Q65R
WT
REAF/Ponceau S ADU of relative level
Time p.i. (hours)

781

782

783 **Figure 2: Fluctuations in subcellular REAF expression after HIV-1 infection are Vpr**
784 **dependent. (A)** Nuclear and cytoplasmic REAF mean fluorescence intensity (MFI) in MDMs
785 measured by imaging flow cytometry. Error bars represent standard deviations of means of
786 replicates. **(B)** Nuclear REAF MFI in indicated primary cell types measured by imaging flow
787 cytometry. Error bars represent standard deviations of means of two blood donors. **(C)** REAF
788 protein in MDMs treated with empty or Vpr-containing VLPs. GAPDH is a loading control. VLP
789 input was equivalent at 100ng of p24. **(D)** Percentage (%) change in subcellular REAF MFI in
790 MDMs from time '0' measured by imaging flow cytometry after challenge with HIV-1 89.6^{WT} or
791 HIV-1 $89.6^{\Delta vpr}$. Data from two donors are presented. **(E)** Infectivity (FFU/ml) of HIV-1 89.6^{WT} in
792 MDMs transfected with siRNA-REAF. HiPerfect (transfection reagent) and siCB are negative
793 controls. ** = P<0.01, *ns* = not significant, one-way ANOVA and *post hoc* Dunnett's test. **(F)**
794 Infectivity of HIV-1 89.6^{WT} compared with HIV-1 $89.6^{\Delta vpr}$ and HIV-1 89.6^{F34I} in MDMs. p24
795 antigen concentrations over 28 days post infection are indicated. Viral input was equivalent at
796 50ng of p24. Error bars represent standard deviations of means of duplicates (*** = P < 0.001;
797 **** = P < 0.0001, two-way ANOVA; the same results were obtained for HIV-1 89.6^{WT} versus
798 HIV-1 $89.6^{\Delta vpr}$ and HIV-1 89.6^{F34I}). Data is representative of at least two independent
799 experiments. **(G)** Percentage (%) change in total cellular REAF MFI from time '0' in MDMs after
800 challenge with HIV-1 89.6^{WT}, HIV-1 $89.6^{\Delta vpr}$ or HIV-1 89.6^{F34I}. Results are representative of three
801 independent experiments. **(H)** REAF protein, measured by Western blotting, in MDMs challenged
802 with HIV-1 89.6^{WT} **or** HIV-1 89.6^{Q65R} over time. Ponceau S staining of nitrocellulose membrane
803 is a loading control. Associated densitometry is presented in **(I)** where error bars represent standard
804 deviations of means where analysis was performed in triplicate.
805

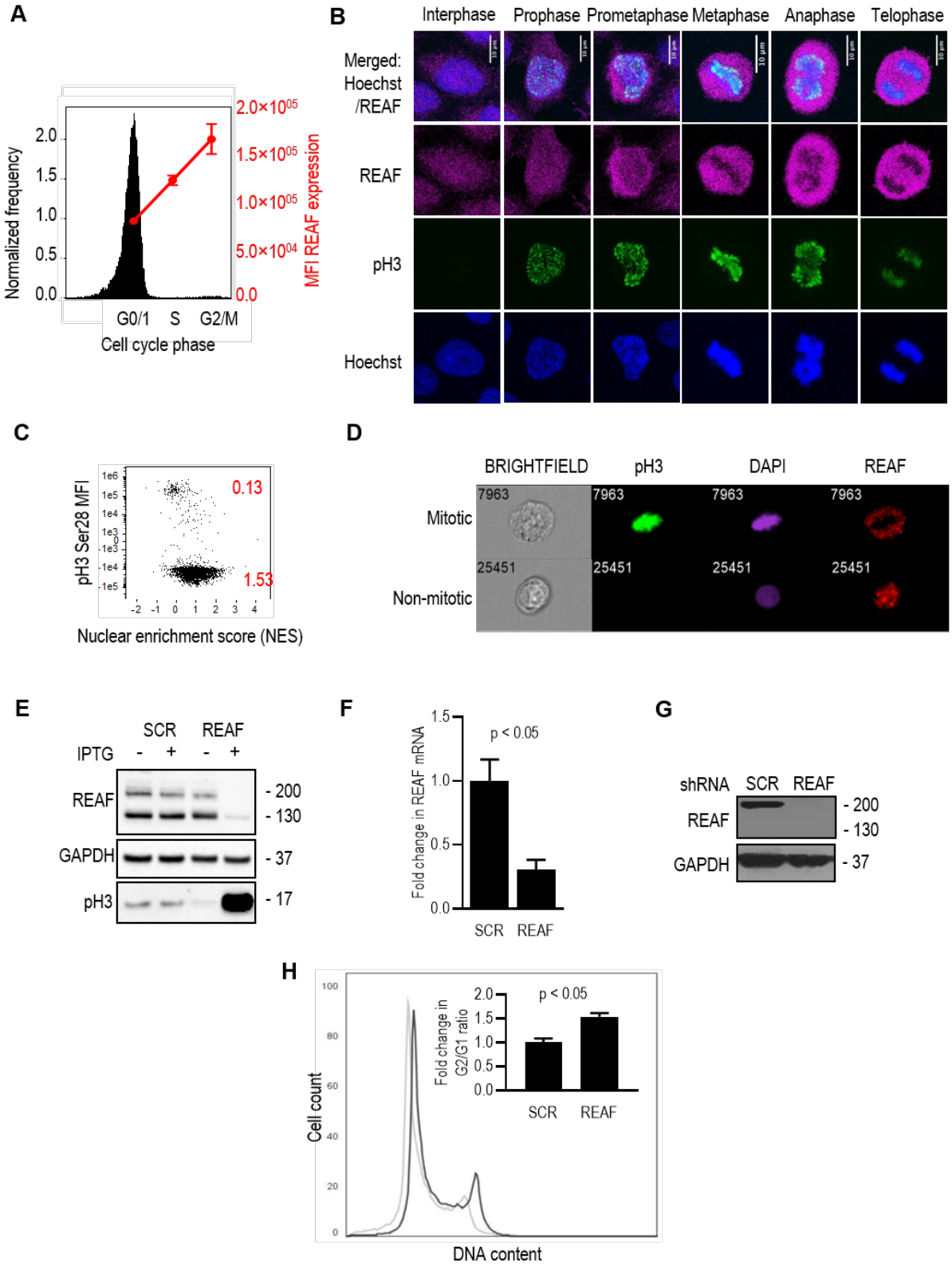
A
Normalized frequency
2.0
1.5
1.0
0.5
0.0
2.0×10^05
1.5×10^05
1.0×10^05
5.0×10^04
0.0
MFI REAF expression
G0/1
S
G2/M
Cell cycle phase
B
Interphase
Prophase
Prometaphase
Metaphase
Anaphase
Telophase
Merged: Hoechst /REAF
REAF
pH3
Hoechst
C
pH3 Ser28 MFI
0.13
1.53
Nuclear enrichment score (NES)
D
BRIGHTFIELD
pH3
DAPI
REAF
Mitotic
Non-mitotic
7963
25451
E
SCR
REAF
IPTG
- + - +
REAF
GAPDH
pH3
- 200
- 130
- 37
- 17
F
p < 0.05
Fold change in REAF mRNA
1.5
1.0
0.5
0.0
SCR
REAF
G
shRNA
SCR
REAF
REAF
GAPDH
- 200
- 130
- 37
H
Cell count
100
80
60
40
20
0
DNA content
p < 0.05
Fold change in G2/G1 ratio
2.0
1.5
1.0
0.5
0.0
SCR
REAF

806

807

808 **Figure 3: Depletion of REAF results in G2/M accumulation (A)** Imaging flow cytometry of
809 cell cycle phase and REAF protein in DAPI stained primary monocytes **(B)** Confocal microscopy
810 of subcellular REAF in HeLa-CD4. Phospho-histone H3 (Ser28) staining and chromatin
811 morphology (Hoechst 33342) were used for cell cycle phase identification. **(C)** Imaging flow
812 cytometry of subcellular REAF in cycling HeLa-CD4. A lower nuclear enrichment score (red)
813 indicates a lower proportion of overall REAF in the nucleus. Phospho-histone H3 (Ser28) staining
814 confirmed mitotic cells had a lower score of 0.13. **(D)** Representative images of subcellular REAF
815 in mitotic and non-mitotic cells. **(E)** REAF protein in THP-1 with IPTG-inducible shRNA
816 targeting REAF (shREAF) or a scrambled control sequence (shSCR). Phospho-histone H3
817 (Ser10/Thr11) is a mitotic marker and GAPDH is a loading control. (**F)** Fold change in mRNA
818 transcript level in PM1 shREAF normalized to PM1 shSCR measured by qPCR **(G)** REAF protein
819 in PM1 expressing shRNA targeting REAF (shREAF) and PM1 expressing a scrambled control
820 sequence (shSCR). GAPDH is a loading control. **(H)** Flow cytometry of cell cycle phase in PI
821 stained PM1 shREAF (black outline) and PM1 shSCR (grey outline). Plot shown is representative
822 of three biological replicates. Insert shows fold change in G2/G1 ratio in PM1 shREAF normalized
823 to PM1 shSCR. Error bars represent standard deviations of means of three biological replicates.
824
825
826
827
828
829
830

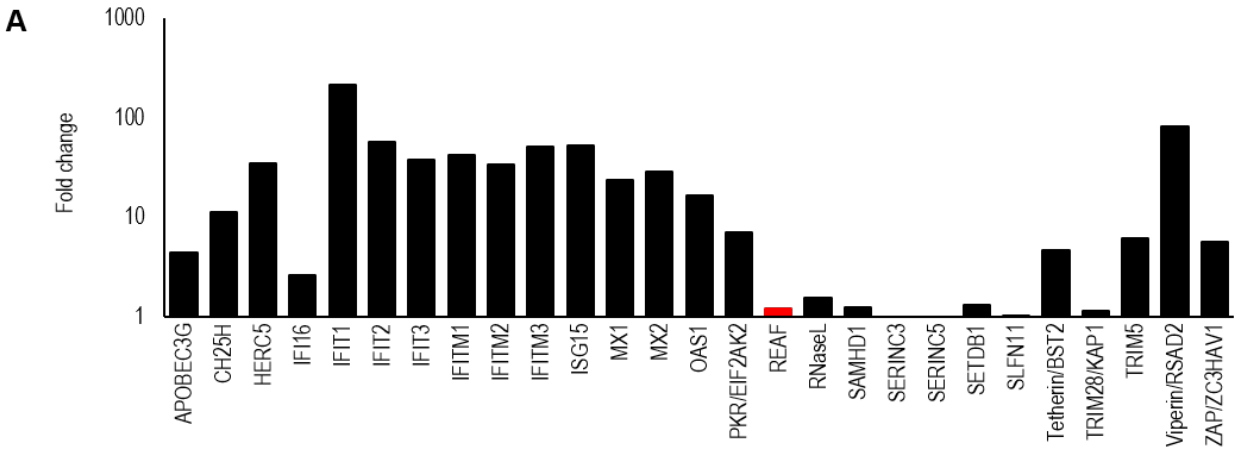

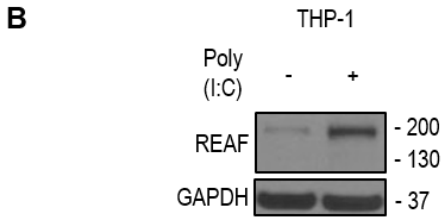

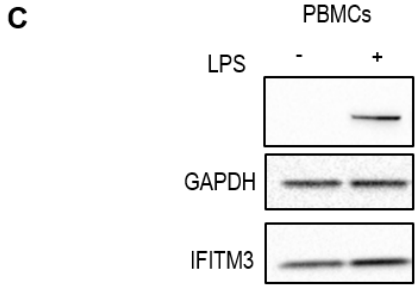

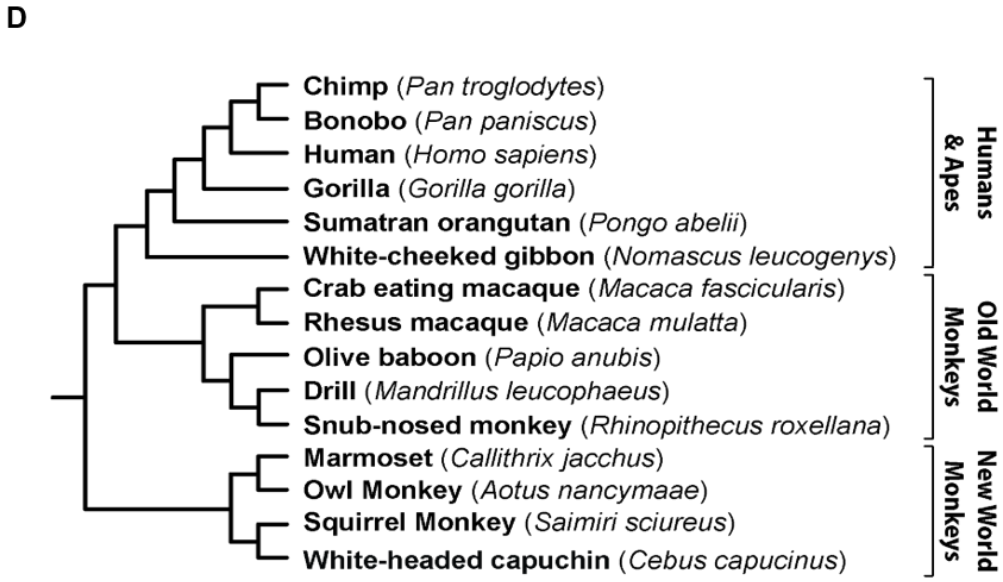

		M1 vs M2		M7 vs M8		M8a vs M8	
Codon freq. model	ω_0	2*ΔlnL	p-value	2*ΔlnL	p-value	2*ΔlnL	p-value
Fcodon	0.4	0.67	0.72	0.95	0.62	0.67	0.41
Fcodon	1.2	0.67	0.72	0.95	0.62	0.67	0.41
F3x4	0.4	0.53	0.86	0.53	0.77	0.32	0.57
F3x4	1.2	0.53	0.86	0.53	0.77	0.32	0.57

832 **Figure 4: REAF is not IFN stimulated or under positive selection. (A)** RNA microarray
833 determined change in REAF mRNA compared to other antiviral factors in MDMs treated with
834 IFNα (500IU/ml). **(B)** REAF protein in PMA differentiated THP-1 after poly(I:C) treatment for
835 48 hours. GAPDH is a loading control. **(C)** REAF protein in PBMCs after LPS treatment. GAPDH
836 is a loading control and IFITM3 is a positive control for LPS induced upregulation. **(D)** REAF
837 DNA sequences from 15 extant primate species (tree length of 0.2 substitutions per site along all
838 branches of the phylogeny) (top) were analyzed using the PAML package for signatures of positive
839 natural selection (bottom). Initial seed values for ω (ω_O) and different codon frequency models
840 were used in the maximum likelihood simulation. Twice the difference in the natural logs of the
841 likelihoods (2*InL) of the two models were calculated and evaluated using the chi-squared critical
842 value. The p value indicates the confidence with which the null model (M1, M7, M8a) can be
843 rejected in favor of the model of positive selection (M2, M8).
844
845
846
847
848
849
850
851
852
853
854